TECHNICAL ARTICLE

Simple preparation of specimens for X-ray powder diffraction analysis of radioactive materials: an illustrative example on irradiated granite

Claudia Aparicio ⓘ,[a] Vít Rosnecký, and Patricie Halodová
Department of Material Analysis, Centrum výzkumu Řež s.r.o. (CVŘ), Hlavní 130, 250 68 Husinec, Czech Republic

Materials in a high radioactive environment undergo structural changes. X-ray diffraction (XRD) is commonly used to study the micro-structural changes of such materials. Therefore, a safe procedure is required for the preparation of specimens. In this paper, a simple methodology for the preparation of radioactive powder specimens to be analyzed in a non-nuclearized laboratory diffractometer is presented. The process is carried out inside a shielded glove box, where the milling of the radioactive sample and specimen preparation occurs. Minimum amount of sample is required (<20 mg), which is drop-casted on a polyether ether ketone (PEEK) foil and glue-sealed inside a disposable plastic holder for a safe handling of the specimen. One example using neutron-irradiated granite is shown, where unit-cell parameters and crystal density of the main phases were calculated. The developed methodology represents an easy and affordable way to study neutron irradiated materials with low activity at laboratory scale.

I. INTRODUCTION

Construction materials in nuclear facilities are constantly under the effects of irradiation (neutron and gamma) and temperature induced by irradiation. The irradiation induces defects and changes in the structure of construction materials. Thus, it is important to evaluate the microstructural changes induced by neutron irradiation that might affect the mechanical properties of materials at macroscale, affecting its performance. X-ray diffraction (XRD) is a widely used technique for structural characterization of materials in a bulk or powder form. Special care must be taken when manipulating radioactive material, especially in a powder form, since it can lead to unwanted radioactive exposure or contamination of personnel (Metcalf and Winters, 1975; Schiferl and Roof, 1978). Therefore, the handling and milling of radioactive materials (e.g., minerals-rocks and concrete) is carried out inside of a hermetically sealed shielded glovebox under negative pressure.

Radioactive samples for XRD analysis must fulfill two requirements: (1) small size to avoid excessive irradiation of the operator and equipment and (2) a containment barrier between the sample and its surroundings to avoid radioactive contamination due to leaking of powder. Different approaches have been used to fulfill those requirements. In some laboratories, the whole diffractometer is inside a glove box, where the sample preparation and measurement are carried out under nitrogen atmosphere (Belin et al., 2015), others developed a sample stage dedicated for irradiated samples (Vauchy et al., 2021). Inspired by holders for air-sensitive samples (Ritter, 1988; Rink et al., 1994; Rodriguez et al., 2008), other authors designed a holder to enclose the sample avoiding the powder exchange with the external atmosphere. Mylar (Belin et al., 2004; Ao et al., 2007) or Kapton (Strachan et al., 2003; Sprouster et al., 2018) was often used as X-ray window. In few cases, the powder samples were mixed with a binding material as resin to avoid dispersion of the radioactive powder into the air (Belin et al., 2004).

To simplify the procedure of specimen preparation, instead of a full metal holder, a disposable plastic insert (commercially available) was chosen, where the sample can be enclosed between two X-ray transparent foils, like the holder used by Sprouster et al. (2018). The advantage of this, is that the low-activity specimen can be stored for future analysis and afterward easily discarded as a radioactive waste without opening the insert, reducing the risk of release of powder and radioactive contamination.

II. EXPERIMENTAL

A. Description of the post-irradiation examination facility at CVŘ

The preparation room of irradiated materials for post-irradiation examination (PIE) is located at the hot cell facility

---

[a] Author to whom correspondence should be addressed. Electronic mail: claudia.aparicio@cvrez.cz

at CVŘ (Husinec-Řež, near Prague, Czech Republic). At the preparation room, there are three shielded glove boxes (produced at CVŘ), which are connected to an independent ventilation system for radioactive materials (active air conditioning). The produced radioactive liquid waste is collected in polyethylene containers. The boxes are made from low-carbon steel (thickness=10 cm) with a radiation shielding window of lead glass and they are kept under negative pressure (-90 to -120 Pa). One of the boxes is dedicated to the preparation of metallographic specimens; and the other two are dedicated to the preparation of specimens from irradiated geological samples, building materials and ceramics. Polishing, grinding, and milling of radioactive samples are carried out inside those boxes. A small semi-shielded glove box is used to label and seal the holders containing the irradiated specimens (Zoul et al., 2021).

B. Radiological safety and waste management during and after specimen preparation

The present study focuses on low-level activity or low radiation level samples (contact dose rate on sample <1 mSv/h). Manipulation of the radioactive samples is done only by radiation workers trained in radiation protection. During the sample milling and specimen preparation, the worker must wear clothes only to be used at controlled areas, lab coat, rubber gloves, lab goggles, and a half-mask respirator with filters. An electronic dosimeter is worn to monitor the dose rate. Sample milling and specimen preparation must be performed inside a glove box. All the disposable objects after specimen preparation used inside the glove box become solid radioactive waste.

The prepared specimen is transported to the XRD lab inside a lead-shielded steel container. After loading the specimen into the container, dose equivalent rate on the surface of the container must be measured and it should not exceed 1 μSv/h. Monitoring the contamination on the surface of the container and on the worker must be performed before leaving the controlled area (hot-cell facility).

In case of contamination, inside the glove box or diffractometer, we must clean up any radioactive powder using a wet cellulose tissue, being careful to not expand the contaminated area, then cleaning the surface with absolute ethanol, continue until the values registered by the surface contamination detector are ≤ 0.4 Bq/cm^2 for β and γ radiation or ≤ 0.04 Bq/cm^2 for α radiation.

After XRD measurements, the specimens are taken back to the glove box, where they are removed from the metallic ring holder, keeping the plastic holder sealed. Then, they are stored in a small polyethylene container. The specimens inside the container are considered a non-compactable radioactive waste and they are sent to the radioactive-waste handling centre, where they manage their final disposal.

C. Milling of the solid sample and specimen preparation for XRD analysis

Powder preparation from the bulk sample (a cylinder with a 1 cm height and 1 cm diameter) and subsequent preparation of specimens for XRD were carried out inside a shielded glove box (Figures 1(a) and 1(b)). The powder was prepared using an oscillating ball mill, model MM400 (Retsch, Germany), equipped with two stainless steel milling jars (35 ml) with zirconium oxide (ZrO$_2$) inner coating and zirconium oxide balls (diameters of 10 and 20 mm) (Figure 1(c)). "Wet" milling was chosen because it offers the advantage to produce a powder with a homogeneous size distribution and to reduce the risk of dispersion of radioactive dust in the glove box. Three steps were followed for the milling of the bulk sample in ethanol: (1) fast grinding to break down the bulk sample into a
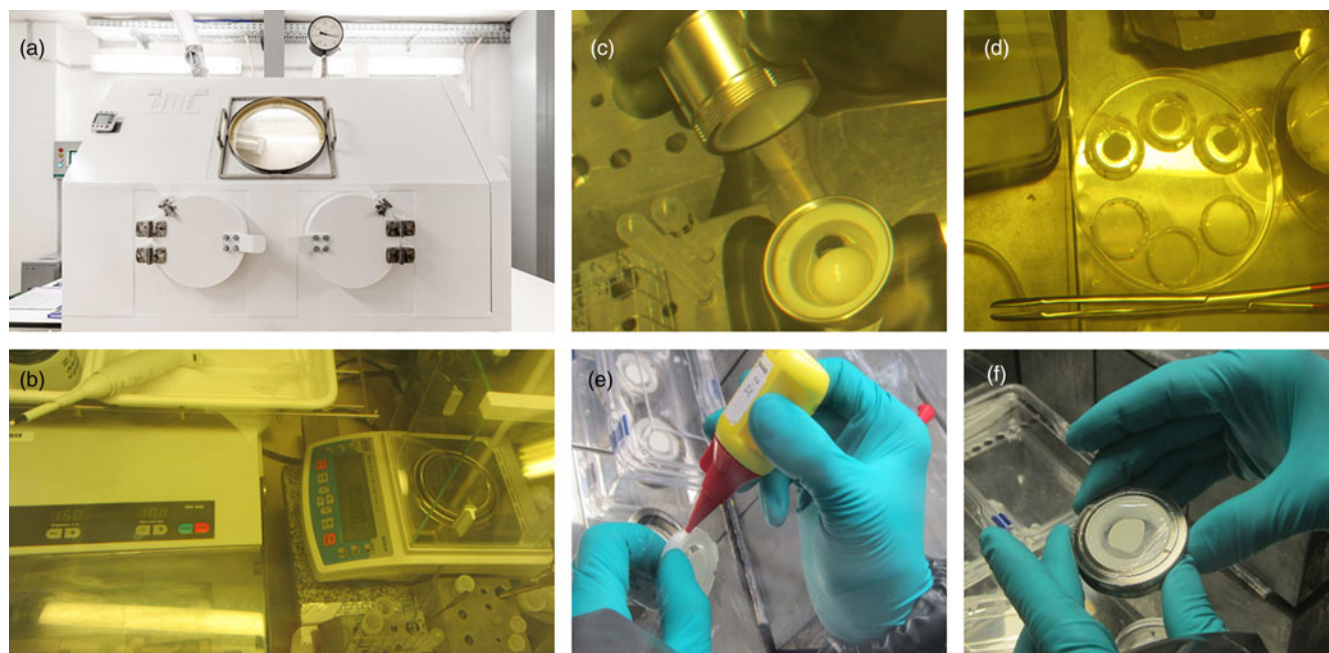

Figure 1. Preparation of specimen for XRD analysis. (a) Shielded glove box where the specimens are prepared; (b) inside of the glove box, on the left is the oscillating mill and micropipette, on the right a weighing scale; (c) insertion of the bulk sample and ZrO$_2$ ball to the milling jar; (d) drying of the drop-casted samples before closing the plastic holder; (e) sealing of the plastic holder containing the radioactive sample; and (f) specimen ready for XRD analysis.

coarse powder (one 20 mm ZrO_2 ball, 20 Hz, 1.5 min); (2) first cycle of "wet" milling to reduce the size of the particles in the powder (two 10 mm ZrO_2 balls, 20 Hz, 10 min); (3) second cycle of "wet" milling with lower oscillation frequency to homogenize the size distribution of the particles in the powder (two 10 mm ZrO_2 balls, 15 Hz, 10 min), thus producing a fine powder. Using this method, a mean particle size of $2.80 \pm 0.05 \, \mu m$ was achieved, the value is a result of fitting the data set of independent measurements to a lognormal distribution. The use of ethanol (2 ml) as a wet medium reduces the friction between the particles, therefore more homogeneous and rounded particles with narrower size distribution are produced (Sathiyakumar and Gnanam, 2002). After the milling, the resulting slurry was poured into a labelled polystyrene vial, and it was air-dried at room temperature.

The XRD specimens were prepared by drop-casting of the sample (approx. 15 mg) with a micropipette onto a polyether ether ketone (PEEK, 6 µm, BIEGLO GmbH) foil fixed to a disposable plastic transmission holder (bought from Malvern-Panalytical). After drying, the sample is covered with a second PEEK foil (Figure 1(d)). The reason for choosing PEEK over Mylar foil is that it does not show diffraction peaks in the region of interest during the XRD measurements (Figure 2). The specimen enclosed between foils inside the plastic holder is then transferred to the semi-shielded glove box, there the plastic holder is sealed with polyvinyl acetate glue (Figure 1(e)) before its insertion into the metallic holder (Figure 1(f)). The sealing of the two rings secures the active specimen inside the internal holder preventing any powder leaking. Now the specimen is ready for transport, in a shielded container, to the room where the XRD measurement is performed.

D. XRD measurement of the radioactive specimens

The data collection was performed at room temperature using a non-nuclearized multipurpose diffractometer (Empyrean, Malvern-PANalytical) with a Co X-ray tube (Co-$K\alpha$1, $\lambda = 1.7890$ Å, generator settings: 40 kV, 40 mA, line focus) in transmission mode. An elliptic focusing mirror, fixed divergence
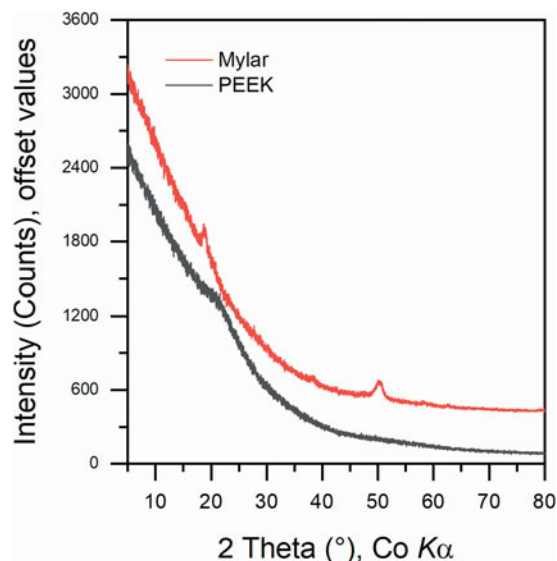

Figure 2. Diffraction patterns of Mylar and PEEK foils in transmission geometry. Mylar pattern is shifted upwards for better clarity.

slit 1/2°, fixed anti-scatter slit 1/2°, and Soller slit of 0.02 rad were used in the incident beam. A PIXcel3D detector (1D mode) attached to a new optical module dCore containing a programmable anti-scatter slit (fixed mode 1/2°) and Soller slit (0.02 rad) were used in the diffracted beam. All patterns were collected in the angular range from 4° to 82° 2θ with a step size of 0.013° 2θ. For the Mylar, PEEK, and LaB$_6$ samples scan speed of 0.022 °/s was used. For the radioactive samples, a scan speed of 0.010 °/s was used. The diffractometer possesses a magazine and a robotic arm for automatic loading of specimens, and it can be operated remotely reducing the exposure of the operator to radiation. Data analysis and Rietveld refinement was performed using Profex 5.2.2 software package (Döbelin and Kleeberg, 2015), the crystal structural models were taken from the Profex internal database (*.str files, freely available from http://www.bgmn.de/download-structures.html) and PDF-4+ database (Gates-Rector and Blanton, 2019).

E. Correct assembly of the inner plastic holder for specimen preparation

Given that the correct position of the specimen in the center of the goniometer is an important requirement, especially when the data are used for determination of unit-cell parameters, tests were performed to find the best position of the sample in the plastic holder.

The disposable plastic holders are composed of four separated pieces, the bottom part consists of a base and a ring to keep in place the PEEK foil, and the top part consist of two rings, the internal ring has a smooth surface, and the external ring has three legs (Figure 3(a)). There are two possibilities of assembly the top part, either with the external ring with the "legs up" or the "legs down" (Figures 3(b) and 3(c)). To observe whether it affects the position of the peaks of a given sample, one specimen for each assembly was prepared, using hexaboride lanthanide LaB$_6$ (SRM660c NIST-certified standard) as a testing sample. Both specimens were measured in transmission mode using the configuration described in the previous section.

After the measurement, the position of the peaks of both specimens were compared with the certified values of LaB$_6$ (NIST, 2015), those values are listed in the Table I. From the table, there is a visible difference between the 2θ position of peaks from both assemblies up to 0.020° at higher angles. In the 2θ range of measurement, the assembly with "legs down" has less deviation from the certified values, therefore it was used when preparing specimens of radioactive samples.

Additional test has been performed to observe the variation of the 2θ peaks position with the repeated insertion of the plastic holder into the metallic ring holder, the action was repeated five times using the LaB$_6$ standard as a reference. The measured 2θ values are listed in the Table II, where the variability of the peaks position due to insertion is minimal, with a deviation of $\pm0.003°$ from the certified 2θ values.

III. CASE STUDY: NEUTRON-IRRADIATED GRANITE

The studied sample was granite rock from Hästholmen (Finland) containing quartz (34%), plagioclase (19.5%), potassium feldspar (38.5%), biotite (5%), hornblende (2%), and chlorite (1%) as reported by mineralogical analysis.
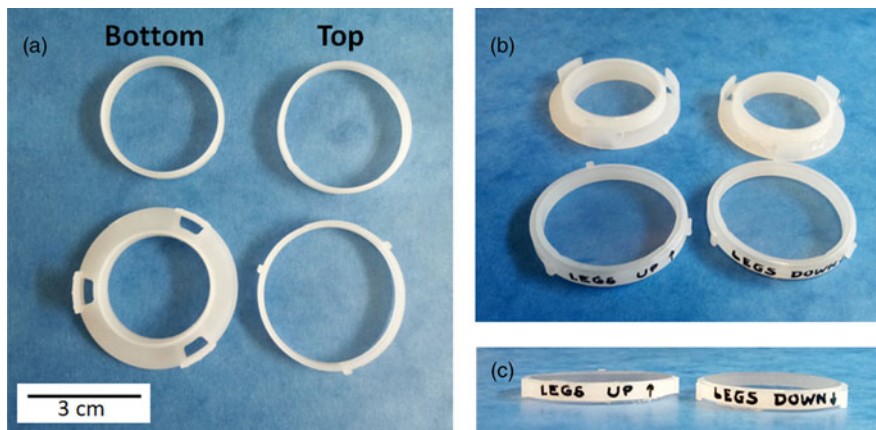
Figure 3. Disposable plastic holder. (a) Disassembled pieces before the adding of PEEK foil, (b) partially assembled holders with the fixed PEEK foil, showing the assemblies of the top part with the "legs up" (left) and "legs down" (right), (c) a frontal view of the top part of the holders. The PEEK foil was fixed to the plastic holder by a resin-based adhesive for rigid plastics.

TABLE I. Variation of the peak positions of LaB$_6$ (SRM660c) depending on the assembly of the inner plastic holder during specimen preparation.

Certified peak position 2θ (°)	Legs-up peak position 2θ (°)	Diff. with certified value (°)	Legs-down peak position 2θ (°)	Diff. with certified value (°)	Difference up –down (°)
24.853	24.834	−0.019	24.847	−0.006	0.013
35.435	35.412	−0.023	35.427	−0.008	0.015
43.766	43.744	−0.022	43.760	−0.006	0.016
50.983	50.959	−0.024	50.978	−0.005	0.019
57.524	57.501	−0.023	57.520	−0.004	0.019
63.620	63.596	−0.024	63.616	−0.004	0.020

The certified values of LaB$_6$ peak position are taken from the corresponding certificate of analysis (NIST, 2015).

TABLE II. Variation of the peak positions of LaB$_6$ (SRM660c) after several insertions of the plastic insert into the metallic ring holder.

Certified peak position 2θ (°)	LD-1 peak position 2θ (°)	LD-2 peak position 2θ (°)	LD-3 peak position 2θ (°)	LD-4 peak position 2θ (°)	LD-5 peak position 2θ (°)	LD avg. peak position 2θ (°)	Diff. with certified value (°)
24.853	24.848	24.848	24.850	24.851	24.851	24.850	−0.003
35.435	35.430	35.431	35.432	35.434	35.434	35.432	−0.002
43.766	43.762	43.763	43.765	43.766	43.765	43.764	−0.002
50.983	50.981	50.982	50.983	50.984	50.985	50.983	0.000
57.524	57.524	57.524	57.526	57.526	57.527	57.525	0.001
63.620	63.621	63.622	63.622	63.625	63.625	63.623	0.002

The certified values of LaB$_6$ peak position are taken from the corresponding certificate of analysis (NIST, 2015).
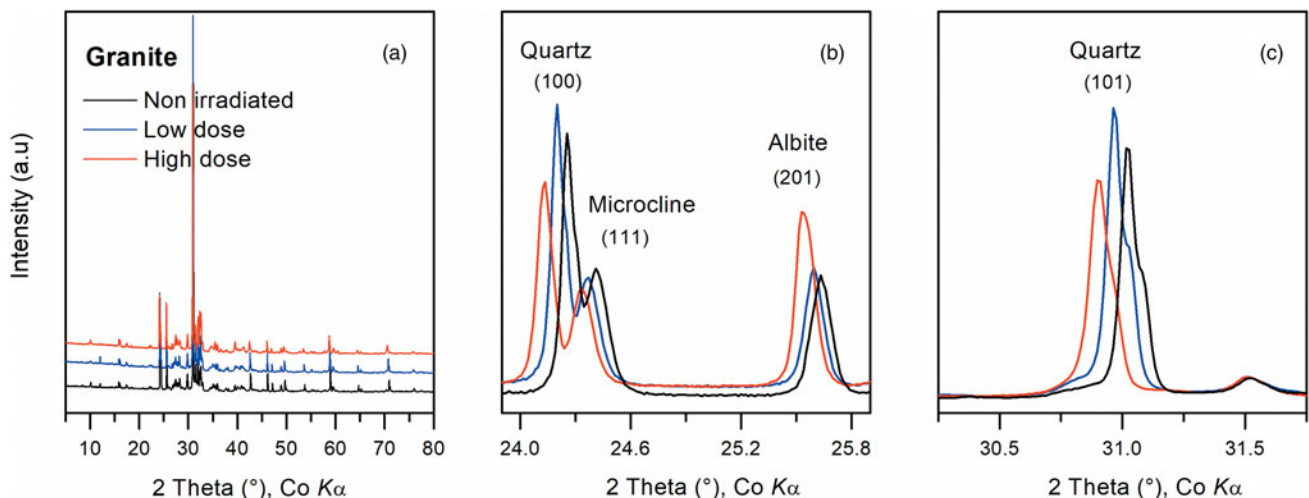

Figure 4. Diffraction patterns of non-irradiated (black line), low-dose (blue line), and high-dose (red line) neutron-irradiated granite (a), where shift to lower angles of the main reflections of quartz (b and c), microcline and albite (b) is evident.
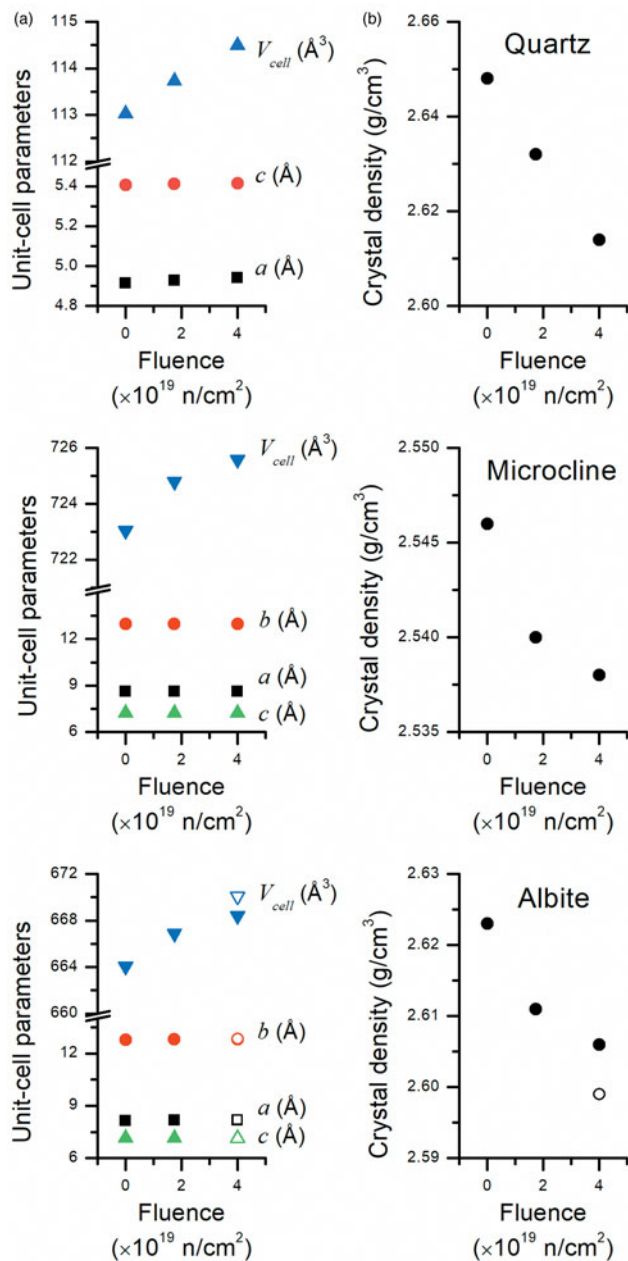
Figure 5. Graphs showing a visible increment of the unit cell (left) and decrease of the crystal density (right) of quartz, microcline, and albite after neutron irradiation. The open symbols in the albite graphs represent an expanded form of albite.

Inside the research reactor LVR-15 at CVŘ, bulk granite samples were exposed to two different neutron fluences: low dose 1.74×10^{19} n/cm^2 and high dose 4×10^{19} n/cm^2 (>0.1 MeV). Specimens from the non-irradiated and irradiated (low and high dose) samples were prepared and afterwards measured in transmission mode using the procedure and settings described in the experimental section.

There is a visible shift of several peaks to lower angles with the increase of the neutron fluence (Figure 4), which is a clear indication of volumetric expansion of unit cells. The unit-cell parameters of the main phases were determined by Rietveld refinement of their corresponding structural models: quartz (space group $P3_221$, quartz.str), microcline (space group C-1, Micromax.str), albite (space group C-1, PDF 04-007-5466).

The results of the refined unit-cell parameters are shown in Figure 5(a). The increase of the unit-cell parameters is more noticeable in the quartz a-axis going from 4.9138(1) Å up to 4.9413(1) Å, for non-irradiated and neutron-irradiated, respectively, giving an increase of the unit-cell volume up to 1.3%. The other two phases affected show a smaller volumetric expansion, being only 0.35% for microcline and 0.65% for albite. However, with higher irradiation dose we found coexisting albite with differently expanded unit cell, being the second albite more expanded, but conserving the same space group, in this case the volumetric expansion reached 0.9%.

Knowing the unit-cell parameters allows the calculation of the crystal density (ρ_c) by using the equation $\rho_c = 1.6604 \cdot (ZM/V_{cell})$, where Z is the number of formula units in the unit cell, M the molecular mass of the formula unit, V_{cell} the unit cell volume in Å^3, and 1.6604 is a conversion factor (Madsen and Scarlett, 2008). The calculated crystal densities are plotted in Figure 5(b). In all cases it is observed a decrease of the crystal density with the increasing neutron fluence, being again the maximum decrease at high dose for quartz (−1.3%), followed by albite (−0.9%) and microcline (−0.3%).

IV. CONCLUSIONS

Following the described mounting and handling procedures, both criteria for handling radioactive samples has been fulfilled, where contention barriers and reduced amount of radioactive sample are used. Therefore, over exposure to radiation during manipulation of the specimens is reduced. Wet milling achieved a homogeneous particle size distribution of powder suitable for XRD analysis, while enclosing the powder sample between X-ray transparent foils prevents the leakage of radioactive dust particles. Correct assembly of the disposable holder offers a reliable specimen positioning in the center of the goniometer, thus reducing the source of error due to misalignment. With the described procedure the phase identification, semi-quantitative analysis, and Rietveld refinement analysis to monitor the changes in unit-cell parameters of the identified crystalline phase can be safely performed on low activity radioactive samples. The method can also be extended to semi-quantitative analysis of amorphous content using the internal-standard method. The presented methodology represents a simplified and affordable way to study irradiated materials at laboratory scale.

CONFLICTS OF INTEREST

The author(s) declare no conflicts of interest.

REFERENCES

Ao, B., Wang, X., Wei, Y., and Zhang, Y. 2007. "A Simple Hermetic Sample Holder for X-Ray Diffraction Analysis of Uranium Hydride." *Journal of Applied Crystallography* 40: 796–98. doi:10.1107/S0021889807024661.

Belin, R. C., Valenza, P. J., Reynaud, M. A., and Raison, P. E. 2004. "New Hermetic Sample Holder for Radioactive Materials Fitting to Siemens D5000 and Bruker D8 X-Ray Diffractometers: Application to the Rietveld Analysis of Plutonium Dioxide." *Journal of Applied Crystallography* 37: 1034–37. doi:10.1107/S0021889804022885.

Belin, R. C., Strach, M., Truphémus, T., Guéneau, C., Richaud, J., and Rogez, J. 2015. "In Situ High Temperature X-Ray Diffraction Study of the Phase Equilibria in the UO_2-PuO_2-Pu_2O_3 System." *Journal of Nuclear Materials* 465: 407–17. doi:10.1016/j.jnucmat.2015.06.034.

Döbelin, N., and Kleeberg, R. 2015. "Profex: A Graphical User Interface for the Rietveld Refinement Program BGMN." *Journal of Applied Crystallography* 48: 1573–80. doi:10.1107/S1600576715014685.

Gates-Rector, S., and Blanton, T. 2019. "The Powder Diffraction File: A Quality Materials Characterization Database." *Powder Diffraction* 34(4): 352–60. doi:10.1017/S0885715619000812.

Madsen, I. and Scarlett, N. (2008). Quantitative Phase Analysis in R. Dinnebier and S. Billinge (Eds.) *Powder Diffraction: Theory and Practice* (pp. 298–331). Cambridge, PSC Publishing.

Metcalf, S. G., and Winters, W. I. 1975. "An X-Ray Diffraction Technique for Radioactive Powders." *Applied Spectroscopy* 29(6):519–21. doi:10.1366/000370275774455635.

National Institute of Standards & Technology. 2015 Standard Reference Material® 660c. Line Position and Line Shape Standard for Powder Diffraction (Lanthanum Hexaboride Powder). https://www-s.nist.gov/srmors/certificates/660c.pdf. Accessed October 31, 2021.

Rink, W. J., Mathias, H. G., and Schlenoff, J. B. 1994. "Hermetic Sample Housing for X-Ray Diffraction Studies." *Journal of Applied Crystallography* 27: 666–68. doi:10.1107/S0021889807024661.

Ritter, J. 1988. "An Hermetically Sealed Inert Atmosphere Cell for X-Ray Powder Diffraction." *Powder Diffraction* 3(1): 30–31. doi:10.1017/S0885715600013087.

Rodriguez, M. A., Boyle, T. J., Yang, P., and Harris, D. L. 2008. "A Beryllium Dome Specimen Holder for XRD Analysis of Air Sensitive Materials." *Powder Diffraction* 23(2):121–124. doi:10.1154/1.2912452.

Sathiyakumar, M., and Gnanam, F. D. 2002. "Influence of Milling Liquids and Additives on Particle Size Reduction and Sintering Behaviour of Al_2O_3." *British Ceramic Transactions* 101(5): 200–7. doi:10.1179/096797802225003974.

Schiferl, D., and Roof, R. 1978. "X-Ray Diffraction of Radioactive Materials." *Advances in X-ray Analysis* 22: 31–42. doi:10.1154/S0376030800016396.

Sprouster, D. J., Weidner, R., Ghose, S. K., Dooryhee, E., Novakowski, T. J., Stan, T., Wells, P., Almirall, N., Odette, G. R. and Ecker, L. E. 2018. "Infrastructure Development for Radioactive Materials at the NSLS-II." *Nuclear Instruments and Methods Physics Research A* 880: 40–5. doi:10.1016/j.nima.2017.10.053.

Strachan, D. M., Schaef, H. T., Schweiger, M. J., Simmons, K. L., Woodcock, L. J., and Krouse, M. K. 2003. "A Versatile and Inexpensive XRD Specimen Holder for Highly Radioactive or Hazardous Specimens." *Powder Diffraction* 18(1): 23–8. doi:10.1154/1.1523078.

Vauchy, R., Fouquet-Métivier, P., Martin, P. M., Maillard, C., Solinhac, I., Guéneau, C., and Léorier, C. 2021. "New Sample Stage for Characterizing Radioactive Materials by X-Ray Powder Diffraction: Application on Five Actinides Dioxides ThO_2, UO_2, NpO_2, PuO_2 and AmO_2." *Journal of Applied Crystallography* 54: 636–43. doi:10.1107/S1600576721002235.

Zoul, D., Koplová, M., Zimina, M., Halodová, P., Zháňal, P., Libera, O., Janura, R and Rosnecký, V. 2021. "Infrastruktura horkých komor Centra výzkumu Řež (4. díl)." *Jaderná Energie*. 2(67), 32–43.